

PAPER • OPEN ACCESS

Topologically protected colloidal transport above a square magnetic lattice

To cite this article: Daniel de las Heras *et al* 2016 *New J. Phys.* **18** 105009

View the [article online](#) for updates and enhancements.

Related content

- [Macroscopic Floquet topological crystalline steel and superconductor pump](#)
Anna M. E. B. Rossi, Jonas Bugase and Thomas M. Fischer
- [Witnessing topological Weyl semimetal phase in a minimal circuit-QED lattice](#)
Feng Mei, Zheng-Yuan Xue, Dan-Wei Zhang *et al.*
- [Topological edge states in two-gap unitary systems: a transfer matrix approach](#)
Clément Tauber and Pierre Delplace

Recent citations

- [Colloidal topological insulators](#)
Johannes Loehr *et al*
- [Macroscopic Floquet topological crystalline steel and superconductor pump](#)
Anna M. E. B. Rossi *et al*



PAPER

Topologically protected colloidal transport above a square magnetic lattice

OPEN ACCESS

RECEIVED

2 August 2016

REVISED

27 September 2016

ACCEPTED FOR PUBLICATION

13 October 2016

PUBLISHED

26 October 2016

Original content from this work may be used under the terms of the [Creative Commons Attribution 3.0 licence](#).

Any further distribution of this work must maintain attribution to the author(s) and the title of the work, journal citation and DOI.

Daniel de las Heras¹, Johannes Loehr², Michael Loenne³ and Thomas M Fischer²¹ Theoretische Physik, Institutes of Physics and Mathematics, Universität Bayreuth, D-95440 Bayreuth, Germany² Experimentalphysik, Institutes of Physics and Mathematics, Universität Bayreuth, D-95440 Bayreuth, Germany³ Mathematik, Institutes of Physics and Mathematics, Universität Bayreuth, D-95440 Bayreuth, GermanyE-mail: thomas.fischer@uni-bayreuth.de

Keywords: colloids, topology, transport, lattice, four-fold symmetry

Abstract

We theoretically study the motion of magnetic colloidal particles above a magnetic pattern and compare the predictions with Brownian dynamics simulations. The pattern consists of alternating square domains of positive and negative magnetization. The colloidal motion is driven by periodic modulation loops of an external magnetic field. There exist loops that induce topologically protected colloidal transport between two different unit cells of the pattern. The transport is very robust against internal and external perturbations. Theory and simulations are in perfect agreement. Our theory is applicable to other systems with the same symmetry.

1. Introduction

Controlling the transport of colloidal particles is a requisite in several applications such as lab-on-a-chip devices [1], drug delivery with colloidal carriers [2, 3], and computation with colloids [4].

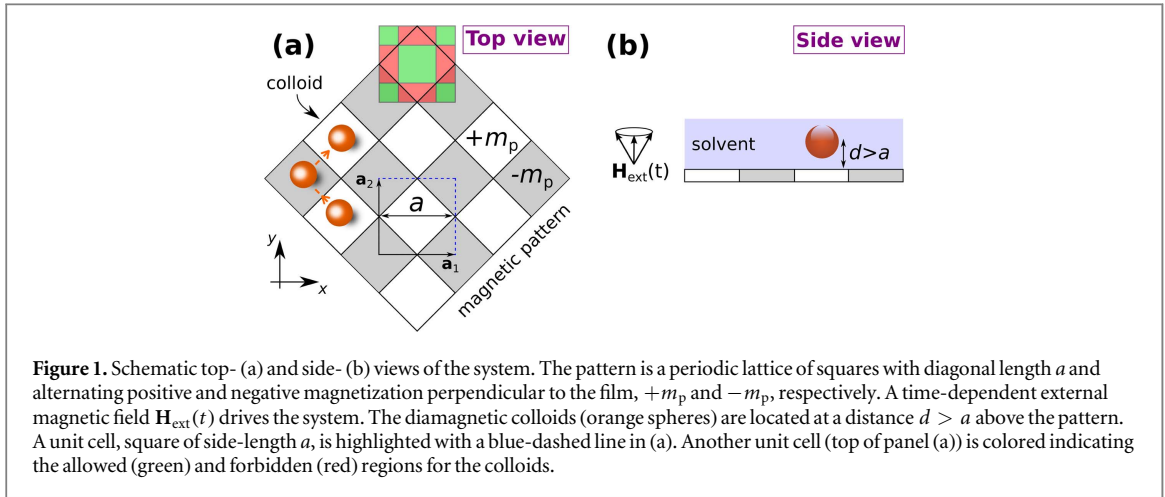
Techniques to control the motion of colloids include the use of gradient fields [5], thermal ratchets [6–8], liquid crystal-based solvents [9, 10], and active particles [11]. Colloidal particles are usually polydisperse in e.g. size, mass, etc. Therefore, the transport of a collection of colloids using the above techniques results always in a dispersion of the motion. One can avoid this by using optical tweezers [12] but at the expenses of having to move the colloids on a one-by-one basis.

Topological protection is a promising tool to overcome these problems. If the dynamics depends only on a topological invariant it is possible to have total control over the colloidal motion, independently of the intrinsic characteristics of the particles. Recently, we have studied the motion of magnetic colloids above a hexagonal magnetic pattern [13]. The system is driven by an external magnetic field. The positions of the colloids above the pattern are given by the minima of the magnetic potential which has contributions from the static field of the pattern and the time dependent external field. The set of stationary points of the potential form a surface in the full phase space whose topological properties fully determine the colloidal motion. There exist transport modes that are topologically protected and therefore extremely robust against perturbations.

The topology of the stationary surface, and hence the topologically protected transport modes, are unique for each type of lattice. Here, we theoretically study the transport of diamagnetic colloidal particles above a square magnetic lattice, and compare the results with computer simulations.

2. Theory

The colloids move in a plane at a distance $d > a$ above the pattern, with a the side-length of the unit cell of the pattern, see figure 1. A time-dependent external magnetic field $\mathbf{H}_{\text{ext}}(t)$ drives the system. The variation in time of $\mathbf{H}_{\text{ext}}(t)$ is slow enough such that the colloidal particles can adiabatically follow the minima of the magnetic potential at any time t . The magnetic potential is $V = -\chi_{\text{eff}} \mu_0 \mathbf{H} \cdot \mathbf{H}$, where \mathbf{H} is the total magnetic field with



contributions from the square pattern and the external potential, $\chi_{\text{eff}} < 0$ is the effective magnetic susceptibility of the diamagnets in the solvent, and μ_0 is the vacuum permeability.

\mathbf{H} can be expressed as a Fourier series with Fourier modes that decay exponentially with z . Hence, at high elevations, $z > a$, the potential is well approximated by $V \propto \mathbf{H}_{\text{ext}}(t) \cdot \mathbf{H}_p(\mathbf{x}_A)$, where

$$\mathbf{H}_p(\mathbf{x}_A) \propto \sum_{i=1}^4 \begin{pmatrix} q_{i,x} \sin(\mathbf{q}_i \cdot \mathbf{x}_A) \\ q_{i,y} \sin(\mathbf{q}_i \cdot \mathbf{x}_A) \\ q \cos(\mathbf{q}_i \cdot \mathbf{x}_A) \end{pmatrix}, \quad (1)$$

is, up to a multiplicative constant, the contribution from the magnetic pattern. Here,

$$\mathbf{q}_i = \frac{2\pi}{a} \begin{pmatrix} \sin(2\pi i/4) \\ -\cos(2\pi i/4) \end{pmatrix}, \quad i = 1, \dots, 4, \quad (2)$$

are the reciprocal lattice vectors of the second Brillouin zone with $q = 2\pi/a$ their common magnitude.

$\mathbf{x}_A = x_1 \mathbf{a}_1 + x_2 \mathbf{a}_2$ with \mathbf{a}_i the basic lattice vectors of the square pattern (see figure 1), are the coordinates in *action space* \mathcal{A} , i.e., the plane above the pattern in which the colloids move. We vary $\mathbf{H}_{\text{ext}}(t)$ on the surface of a sphere,

$$\mathbf{H}_{\text{ext}} = H_{\text{ext}} (\cos \phi_t \sin \theta_t, \sin \phi_t \sin \theta_t, \cos \theta_t). \quad (3)$$

The set (θ_t, ϕ_t) define our *control space*, \mathcal{C} , see figure 2(a). We measure θ_t with respect to the z axis and ϕ_t with respect to \mathbf{a}_1 . The system is driven with periodic closed loops of $\mathbf{H}_{\text{ext}}(t)$. There exist special loops that induce transport between different unit cells, i.e., when \mathbf{H}_{ext} returns to its initial position the particle is in a different unit cell.

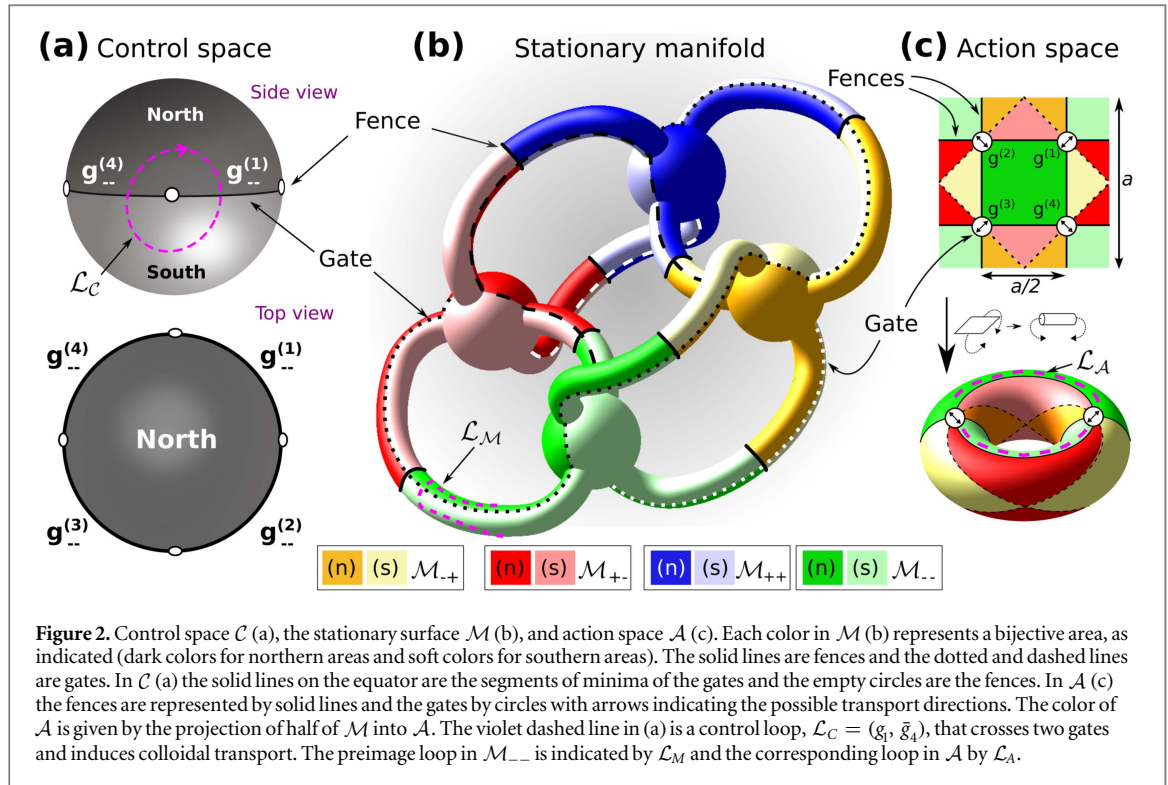
To understand the motion we need to look at the full phase space, i.e., the product space $\mathcal{C} \otimes \mathcal{A}$, with states given by $(\mathbf{H}_{\text{ext}}(t), \mathbf{x}_A)$. The stationary points satisfy $\nabla_{\mathcal{A}} V = 0$, with $\nabla_{\mathcal{A}}$ the gradient in \mathcal{A} . The set of all stationary points is a two-dimensional manifold in $\mathcal{C} \otimes \mathcal{A}$ that we call the *stationary manifold*, \mathcal{M} , see figure 2(b).

The correspondence between \mathcal{M} and \mathcal{C} is not bijective. Each direction of the external field is a point in \mathcal{C} . For each point in \mathcal{C} (with the exception of four special points that we discuss later) there are four points (preimages) in \mathcal{M} , the solutions of $\nabla_{\mathcal{A}} V = 0$. Two solutions are saddle points of V , one is a maximum, and the other one is a minimum. In \mathcal{A} the four points form a square of side $a/2$.

The correspondence between \mathcal{M} and \mathcal{A} is also not bijective. Consider the unit vectors $\hat{\mathbf{e}}_i(\mathbf{x}_A) = \partial_i \mathbf{H}_p / |\partial_i \mathbf{H}_p|$, $i = 1, 2$. Then, a point \mathbf{x}_A in \mathcal{A} is stationary if the external field points in a direction perpendicular to both $\hat{\mathbf{e}}_1$ and $\hat{\mathbf{e}}_2$, i.e.,

$$\mathbf{H}_{\text{ext}}^{(s)}(\mathbf{x}_A) = \pm H_{\text{ext}} \frac{\hat{\mathbf{e}}_1 \times \hat{\mathbf{e}}_2}{|\hat{\mathbf{e}}_1 \times \hat{\mathbf{e}}_2|}. \quad (4)$$

The subscript (s) stands for stationary. That is, each point in \mathcal{A} has two preimages $(\mathbf{H}_{\text{ext}}^{(s)}, \mathbf{x}_A)$ in \mathcal{M} (except for special points that we describe later).



Consider now the matrix of the second derivatives of V evaluated at the stationary field

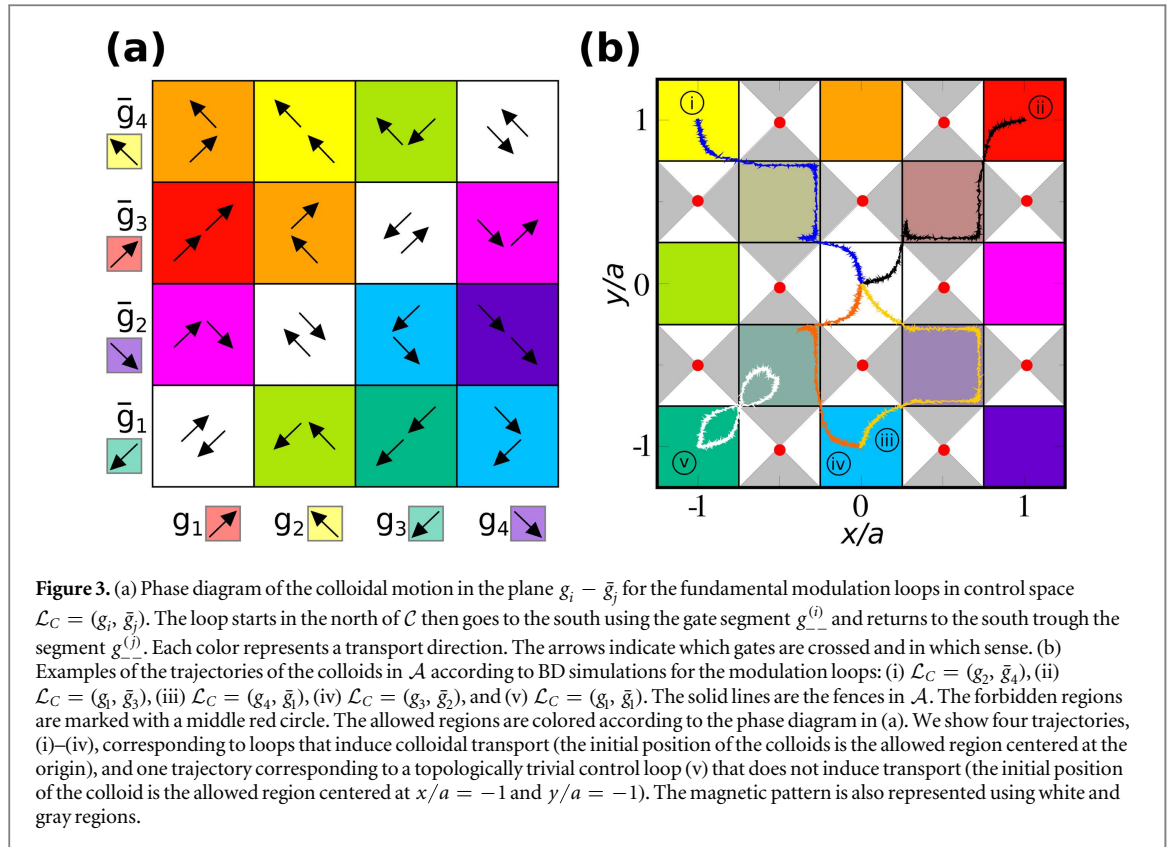
$$\nabla_{\mathcal{A}} \nabla_{\mathcal{A}} V|_{\mathbf{H}_{\text{ext}}^{(s)}} = \begin{pmatrix} \mathbf{H}_{\text{ext}}^{(s)} \cdot \partial_1 \partial_1 \mathbf{H}_p & \mathbf{H}_{\text{ext}}^{(s)} \cdot \partial_1 \partial_2 \mathbf{H}_p \\ \mathbf{H}_{\text{ext}}^{(s)} \cdot \partial_2 \partial_1 \mathbf{H}_p & \mathbf{H}_{\text{ext}}^{(s)} \cdot \partial_2 \partial_2 \mathbf{H}_p \end{pmatrix}, \quad (5)$$

which is diagonal since the mixed derivatives vanish, see (1). The stationary manifold \mathcal{M} is the union of submanifolds $\mathcal{M}_{\alpha\beta}$, where α (β) is the opposite sign of the eigenvalue of (5) with eigenvector pointing in the \mathbf{a}_1 (\mathbf{a}_2) direction. That is, $\mathcal{M} = \mathcal{M}_{++} \cup \mathcal{M}_{+-} \cup \mathcal{M}_{-+} \cup \mathcal{M}_{--}$. Hence the stable trajectories for the colloids reside in \mathcal{M}_{--} (minima of V). \mathcal{M}_{++} are maxima of V , and both \mathcal{M}_{+-} and \mathcal{M}_{-+} are saddle points. All the submanifolds are topologically equivalent since each point in \mathcal{C} has one preimage in each of the submanifolds.

The submanifolds share common borders in \mathcal{M} that we call the *fences*. Any two submanifolds with one common sign of one of the eigenvalues are glued together in \mathcal{M} through two fences. At the fences one eigenvalue changes its sign, i.e., the determinant of (5) vanishes. For example, \mathcal{M}_{++} and \mathcal{M}_{-+} share two fences. At both fences the eigenvalue of the eigenvector pointing along the \mathbf{a}_1 direction changes its sign. The stationary field, equation (4), points along $+\mathbf{a}_2$ in one fence and along $-\mathbf{a}_2$ in the other fence. Hence, in \mathcal{M} we have four submanifolds, and each one is double-joined to other two submanifolds. In other words, \mathcal{M} is a genus 5 surface, see figure 2(b).

Solving $\|\nabla_{\mathcal{A}} \nabla_{\mathcal{A}} V\| = 0$ we can see the fences in action and control space. In \mathcal{C} the fences are four equispaced points along the equator, corresponding to external fields pointing along $\pm\mathbf{a}_1$ and $\pm\mathbf{a}_2$, see figure 2(a). The fences divide action space in a square lattice (length $a/2$) of alternating allowed and forbidden regions, see figure 2(c) and figure 1(a). Using periodic boundary conditions \mathcal{A} is a torus. The allowed regions are areas of minima of V (projection of the submanifold \mathcal{M}_{--} into \mathcal{A}). In the forbidden areas all the stationary points are saddle points. As we have seen, a point in \mathcal{A} can be made stationary with two opposite external fields. Therefore \mathcal{M}_{++} and \mathcal{M}_{--} are projected into the same regions in \mathcal{A} . In other words, if there is a minimum of the potential in a given point in \mathcal{A} we can turn it into a maximum by just pointing the external field in the opposite direction. \mathcal{M}_{+-} and \mathcal{M}_{-+} are also projected into the same areas in \mathcal{A} . In figure 2(c) we show the projection of half of \mathcal{M} into \mathcal{A} (the half that contains all points closer to \mathcal{M}_{--} than to \mathcal{M}_{++}) such that each area has a unique meaning. That is, the projection of this half of \mathcal{M} into \mathcal{A} is bijective.

The fences cross in \mathcal{A} at points that we call the *gates* since they connect two allowed regions in \mathcal{A} . There are four gates $g^{(i)}$, $i = 1, \dots, 4$, see figure 2(c). The gates play a vital role for the colloidal motion. To find the gates in \mathcal{C} we note that the fences do not cross in \mathcal{M} but they do cross in \mathcal{A} . Hence, $\mathbf{H}_{\text{ext}}^{(s)}$ cannot be unique at the gates in \mathcal{A} (crossing points between fences in \mathcal{A}). The only possibility is that $\hat{\mathbf{e}}_1$ is parallel to $\hat{\mathbf{e}}_2$, see equation (4), at the gates. Therefore, as $\mathbf{H}_{\text{ext}}^{(s)} \perp \hat{\mathbf{e}}_1$, $\hat{\mathbf{e}}_2$, the gates in \mathcal{C} are great circles. For the present square lattice the gates in \mathcal{C} are located on the equator. Each gate is divided in four segments, $g_{\alpha\beta}^{(i)}$ where $\alpha, \beta = \pm$ are again the opposite signs



of the eigenvalues of (5). Although all gates in \mathcal{C} are in the equator, they are rotated such that the union of four segments with identical signs of the eigenvalues form a full equator, see figure 2(a).

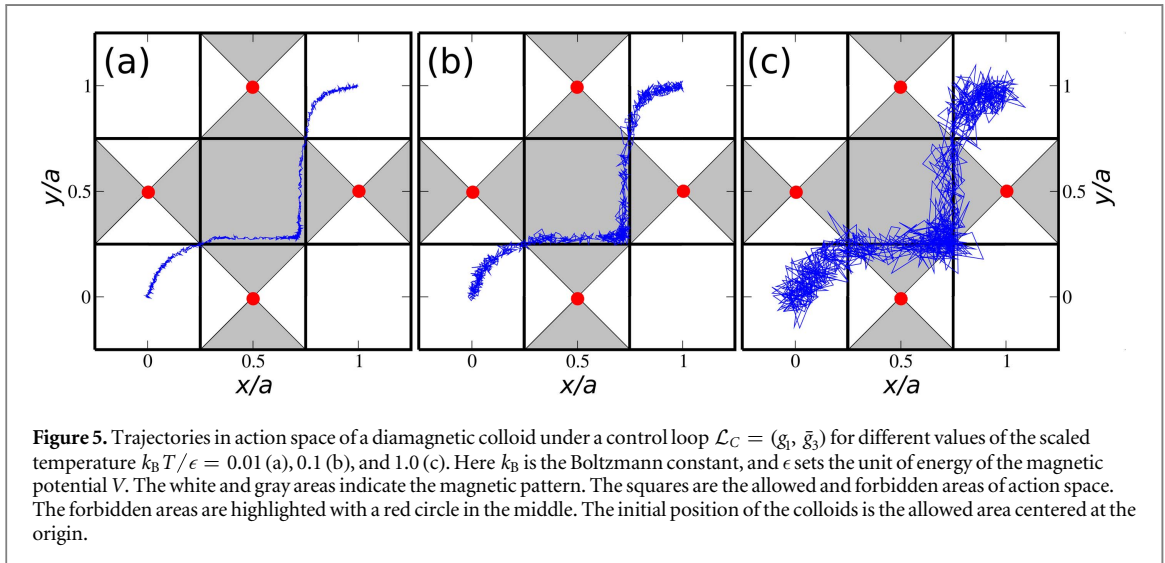
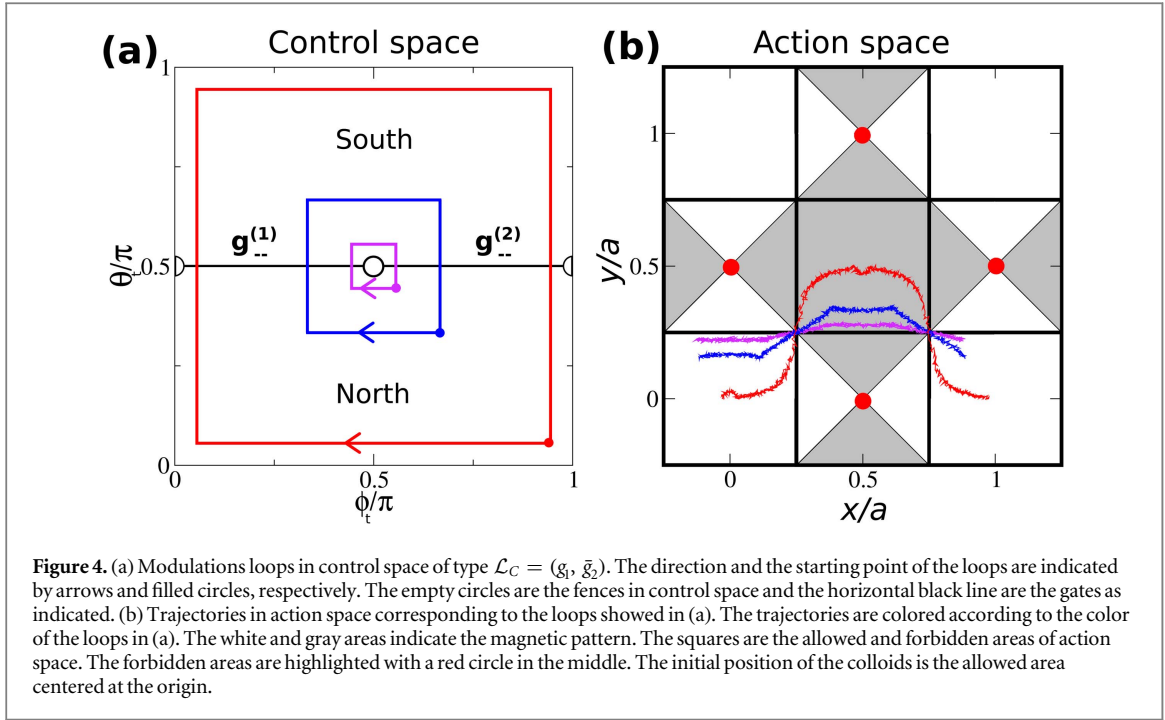
The gates split \mathcal{C} in two parts, the south (s) and the north (n), see figure 2(a). They also split each submanifold of \mathcal{M} in two parts $\mathcal{M}_{\alpha\beta} = \mathcal{M}_{\alpha\beta}^{(n)} \cup \mathcal{M}_{\alpha\beta}^{(s)}$, see figure 2(b). This splitting is very convenient since the resulting regions $\mathcal{M}_{\alpha\beta}^{(\nu)}$ with $\nu = n, s$ are simply connected bijective areas. That is, there are no holes in $\mathcal{M}_{\alpha\beta}^{(\nu)}$ and the correspondences between $\mathcal{M}_{\alpha\beta}^{(\nu)}$ and the other spaces (\mathcal{C} and \mathcal{A}) are unique.

3. Results

We are now in a position to understand the colloidal motion. Let \mathcal{L}_C be a closed modulation loop of the external field in \mathcal{C} . \mathcal{L}_C has four preimage loops in \mathcal{M} , one in each submanifold $\mathcal{M}_{\alpha\beta}$. Only the loop lying in \mathcal{M}_{--} is populated with colloids. This populated loop can be then projected into \mathcal{A} where we can read the actual trajectory of the colloids. Loops \mathcal{L}_C that induce colloidal transport from one unit cell to another in \mathcal{A} are only those that cross at least two different gates in control space, which is equivalent to enclosing at least one fence in \mathcal{C} . When \mathcal{L}_C crosses the segment $g_{-}^{(i)}$ in \mathcal{C} , the corresponding loop that transport the colloids in \mathcal{A} also crosses the gate $g^{(i)}$. Each gate in \mathcal{C} can be crossed from the north to the south or from the south to the north, which in \mathcal{A} results in opposite senses. Let $\mathcal{L}_C = (g_i, \bar{g}_j)$ be a loop of the external field that starts on the north of \mathcal{C} , then goes to the south of \mathcal{C} crossing the segment of minima of the potential of the gate i ($g_{-}^{(i)}$) and returns to the initial point in the north of \mathcal{C} using the segment of minima of the gate j . An example of such a loop is represented in figure 2(a). The phase diagram of the colloidal motion in the $g_i - \bar{g}_j$ plane is depicted in figure 3(a). It has been obtained (i) theoretically by translating loops in \mathcal{C} into loops in \mathcal{A} using the stationary surface \mathcal{M} and (ii) with standard Brownian dynamics simulations. Details of the simulations are provided in the appendix. The agreement between theory and simulations is perfect.

Loops that cross the same gate twice, i.e. $\mathcal{L}_C = (g_i, \bar{g}_i)$, do not induce transport between different unit cells (the initial and the final positions are the same). Loops that cross different gates induce transport between nearest or second nearest unit cells. There are two possible routes for each of the nearest unit cells (see e.g. $\mathcal{L}_C = (g_1, \bar{g}_4)$ and (g_2, \bar{g}_3)) and only one in the case of second nearest unit cells (e.g. $\mathcal{L}_C = (g_1, \bar{g}_3)$). In figure 3(b) we show Brownian dynamics trajectories for selected modulation loops.

The colloidal transport is very robust against internal and external perturbations. The shape of \mathcal{L}_C , for example, is completely irrelevant. Only the gates that \mathcal{L}_C crosses are important. In figure 4 we show the



trajectories in action space for three modulation loops that cross the same two gates, $\mathcal{L}_C = (\underline{g}_1, \underline{g}_2)$, yet following different paths. The trajectories in \mathcal{A} differ but the starting and ending allowed regions are the same. The motion is also robust against changes in the speed of the modulation, the thermal noise, and properties of the colloidal particles such as size, mass, effective susceptibility, etc (see an example in figure 5). Therefore we can transport in a dispersion-free and precise way a collection of particles with a broad distribution of masses, sizes, etc.

The reason behind this robustness is that the transport direction depends only on a topological invariant, and hence it is topologically protected. For each loop in \mathcal{M} we can define a set of 10 winding numbers, two for each hole of \mathcal{M} . $S_{\mathcal{M}}$, the set of winding numbers of the loop in \mathcal{M}_{--} , is the topological invariant. In each of the regions of the phase diagram $S_{\mathcal{M}}$ does not vary. Alternatively we can define the topological invariant of loops in \mathcal{A} and \mathcal{C} . The loop that lies in \mathcal{M}_{--} is projected into a loop in \mathcal{A} and \mathcal{C} . Since \mathcal{M}_{--} is topologically equivalent to control space without the fences, \mathcal{C}' , the correspondence between loops in \mathcal{M}_{--} and \mathcal{C}' is bijective. $S_{\mathcal{C}}$, the set of winding numbers of loops around the fences in \mathcal{C}' induce corresponding winding numbers of loops around the torus in action space ($S_{\mathcal{A}} = \{w_1, w_2\}$ with $w_i = 0, \pm 1$) via the loops in \mathcal{M}_{--} . Each of the eight non-zero values of $S_{\mathcal{A}}$ corresponds to a type of transport in \mathcal{A} . $S_{\mathcal{A}}$ and $S_{\mathcal{C}}$ are also topological invariants, they remain unchanged for each type of transport, i.e, in each region of the phase diagram of figure 3(a).

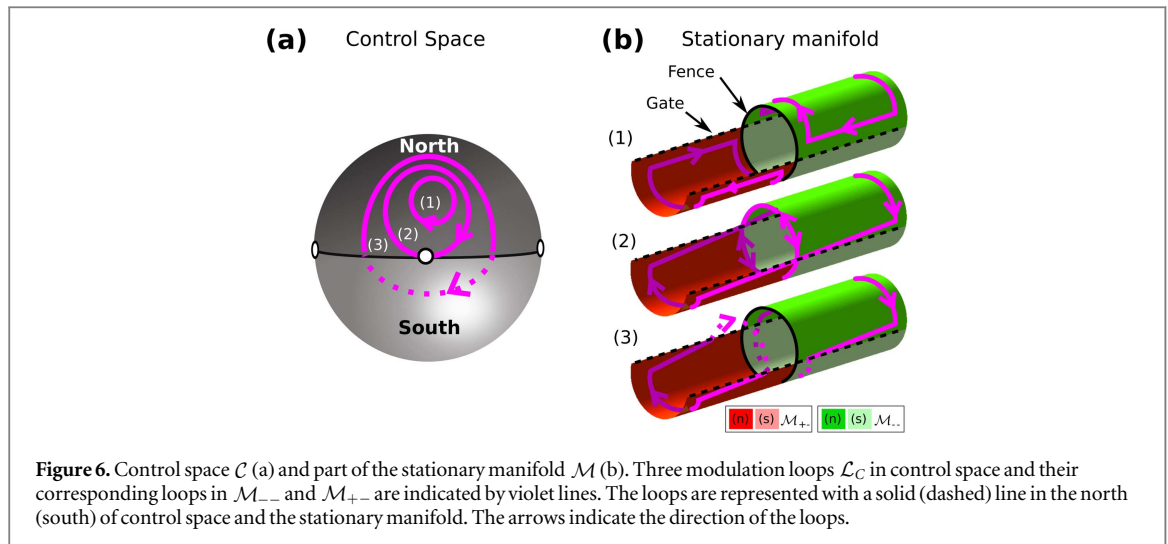


Figure 6. Control space \mathcal{C} (a) and part of the stationary manifold \mathcal{M} (b). Three modulation loops \mathcal{L}_C in control space and their corresponding loops in \mathcal{M}_{--} and \mathcal{M}_{+-} are indicated by violet lines. The loops are represented with a solid (dashed) line in the north (south) of control space and the stationary manifold. The arrows indicate the direction of the loops.

How is it possible to change the direction of transport if it is topologically protected? There are always operations that break the topological protection. This is precisely what happens at the interface between two transport directions in the phase diagram, see figure 3(a). At the interfaces between two different transport modes the topological protection is lost allowing for a change in the transport mode. This occurs for modulation loops that cross at least one of the fences in control space. In figure 6 we show an example of this process. The loop labeled as (1) lies entirely on the north of \mathcal{C} . That is, it does not cross gates and hence does not induce transport between different unit cells. The corresponding loops in \mathcal{M} lie on the northern areas of \mathcal{M} . There is one loop in each of the submanifolds of \mathcal{M} . Figure 6 shows only the loops in \mathcal{M}_{--} and \mathcal{M}_{+-} . When the loop in \mathcal{C} touches one of the fences (see loop (2) in figure 6) the loops in \mathcal{M}_{--} and \mathcal{M}_{+-} join at the fence (the loops in \mathcal{M}_{++} and \mathcal{M}_{-+} also join at a different fence). At this point the colloids, which follow the loop in \mathcal{M}_{--} , have two alternative paths: (i) a loop that resides entirely in the north of \mathcal{M}_{--} and (ii) a loop that lies in both the north and the south of \mathcal{M}_{--} and hence induce colloidal transport between different cells. The motion is not topologically protected in the sense that two different trajectories are possible. Next, we expand the loop in \mathcal{C} such that it encloses one fence in \mathcal{C} and hence crosses two gates, see loop (3) in figure 6. In \mathcal{M} the loops in \mathcal{M}_{--} and \mathcal{M}_{+-} are now disjointed and have interchanged a segment at the fence. The result is two loops that no longer reside in the northern areas of \mathcal{M} . The loop in \mathcal{M}_{--} winds around the holes of \mathcal{M} inducing colloidal transport. The direction of transport has changed with respect to the initial loop (1).

Due to the thermal noise in Brownian dynamics simulations the particles fluctuate around the minima of the potential, exploring the neighborhood of \mathcal{M}_{--} in $\mathcal{C} \otimes \mathcal{A}$. Hence, modulation loops in control space that do not cross a fence, but pass close enough to it, might also be topologically unprotected, leading to two differing transport modes in \mathcal{A} . How close the control loop has to be to the fence in order to be deprotected depends on the magnitude of the thermal noise. The thermal noise effectively expand the fences in \mathcal{C} into the surrounding areas, and broaden the topological transition in \mathcal{A} .

4. Discussion

We have explained the motion of diamagnetic colloids for which the effective susceptibility is negative. Paramagnetic colloids have a positive effective susceptibility, and hence will follow the maxima of V . The minima and the maxima of V always comove in \mathcal{A} separated by $\mathbf{r} = (a/2, a/2)$. Therefore, paramagnetic colloids perform the same motion as diamagnets but displaced by \mathbf{r} .

From an experimental view point, it is possible to use magnetic bubble lattices [14] or lithographic patterns [15] to generate the pattern. Possible methods to levitate the colloids above the pattern consists of using a ferrofluid solvent [13] and the deposition of a polymer layer [16] on the magnetic pattern.

The colloidal transport is fully determined by the topology of the manifold \mathcal{M} , which is unique for each type of magnetic pattern. For example, the stationary manifold of a hexagonal pattern is a genus 7 surface [13]. There, the modulation loops in \mathcal{C} that induce transport of colloids must cross the fences in \mathcal{C} , which are lines instead of points as in the present study. As a result, transport modes of hexagonal and square patterns are completely different. In both, hexagonal and square lattices, the topological invariant in \mathcal{A} is the set of two winding numbers around the hole in \mathcal{A} . This is just a consequence of the dimension of \mathcal{A} . Control space \mathcal{C} neither contains all the information. For example, in square lattices the transition between transport modes occurs for

those loops that cross a fence. However, in hexagonal lattices, a fence crossing loop in \mathcal{C} is a necessary but not sufficient condition to change the transport mode. What fully determines the transport modes is the stationary manifold \mathcal{M} (the topology, the fences, and how \mathcal{M} is projected into \mathcal{A} and \mathcal{C}). In \mathcal{M} the topological invariant is the set of winding numbers around the holes, which is very different in square (\mathcal{M} has genus 5) and hexagonal (\mathcal{M} has genus 7) lattices.

The topologically protected transport modes we have shown here can be understood as bulk modes sustained (driven) by an external field. The transport occurs in the bulk of the periodic system. Other forms of topologically protected motion occur at the edges of a periodic system, such as e.g., the motion of electrons in topological insulators [17], mechanical solitons [18–20], phonons [21], and photons [22, 23] among others. There, a perturbation populates an edge state that cannot scatter into the bulk due to the topology of the system. Our theory is transferable to other systems with the same symmetry. Hence, topological bulk states might exist in e.g. excitons in superlattices [24, 25], tight-binding models [26], and cold atoms in optical lattices [27]. Topologically protected edge states might also occur at the borders of finite magnetic lattices. Their topological properties might be substantially different from those of bulk states. How the edge states in our particle system compare to other edge states in wave systems is a very interesting subject for future studies.

In wave systems, such as e.g. topological insulators, the topology of the band structure is characterized by the Chern numbers of the bands. Each Chern number can be computed as an integral over the Berry curvature of the band [28]. In our particle system we describe the topological protection in terms of the stationary manifold. Both descriptions are probably equivalent in some form.

Acknowledgments

This publication was funded by the German Research Foundation (DFG) and the University of Bayreuth in the funding programme Open Access Publishing.

Appendix. Brownian dynamics simulations

We use Brownian dynamics to simulate the motion of a diamagnetic colloid above the pattern. The coordinates in action space are \mathbf{x}_A , and the equation of motion is given by

$$\xi \frac{d\mathbf{x}_A(t)}{dt} = -\nabla_A V(\mathbf{x}_A, \mathbf{H}_{\text{ext}}(t)) + \boldsymbol{\eta}(t),$$

where t is the time, ξ is the friction coefficient, and $\boldsymbol{\eta}$ is a Gaussian random force with a variance given by the fluctuation-dissipation theorem. The magnetic potential V has contributions from the external field \mathbf{H}_{ext} and the magnetic pattern (see the main text).

The equation of motion is integrated in time with a standard Euler algorithm:

$$\mathbf{x}_A(t + \Delta t) = \mathbf{x}_A(t) - \nabla_A V \Delta t + \boldsymbol{\delta}\mathbf{r}, \quad (\text{A1})$$

where Δt is the time step, and $\boldsymbol{\delta}\mathbf{r}$ is a random displacement sampled from a gaussian distribution with standard deviation $\sqrt{2\Delta t k_B T / \xi}$. Here k_B is the Boltzmann constant, and T is absolute temperature. Before starting the modulation loop in \mathcal{C} we first equilibrate the system by running 10^4 time steps such that the colloids find the minimum of the magnetic potential at $t = 0$.

References

- [1] Gao L, Tahir M A, Virgin L N and Yellen B B 2011 *Lab Chip* **11** 4214
- [2] Kataoka K, Harada A and Nagasaki Y 2001 *Adv. Drug Deliv. Rev.* **47** 113
- [3] Müller R H 1991 *Colloidal Carriers for Controlled Drug Delivery and Targeting: Modification, Characterization and In Vivo Distribution* (London: Taylor and Francis)
- [4] Phillips C L, Jankowski E, Krishnatreya B J, Edmond K V, Sacanna S, Grier D G, Pine D J and Glotzer S C 2014 *Soft Matter* **10** 7468
- [5] Erbe A, Zientara M, Baraban L, Kreidler C and Leiderer P 2008 *J. Phys.: Condens. Matter* **20** 404215
- [6] Matthias S and Müller F 2003 *Nature* **424** 53
- [7] Engel A, Müller H W, Reimann P and Jung A 2003 *Phys. Rev. Lett.* **91** 060602
- [8] Tierno P, Sagues F, Johansen T H and Fischer T M 2009 *Phys. Chem. Chem. Phys.* **11** 9615
- [9] Stark H and Venzki D 2001 *Phys. Rev. E* **64** 031711
- [10] Turiv T, Lazo I, Brodin A, Lev B I, Reiffenrath V, Nazarenko V G and Lavrentovich O D 2013 *Science* **342** 1351
- [11] Jiang H-R, Yoshinaga N and Sano M 2010 *Phys. Rev. Lett.* **105** 268302
- [12] Grier D G 2003 *Nature* **424** 810
- [13] Loehr J, Loenne M, Ernst A, de las Heras D and Fischer T M 2016 *Nat. Commun.* **7** 11745
- [14] Bobeck A H, Bonyhard P I and Geusic J E 1975 *Proc. IEEE* **63** 1176
- [15] Terris B D and Thomson T 2005 *J. Phys. D: Appl. Phys.* **38** R199
- [16] Tierno P and Fischer T M 2014 *Phys. Rev. Lett.* **112** 048302

- [17] Hasan M Z and Kane C L 2010 *Rev. Mod. Phys.* **82** 3045
- [18] Kane C and Lubensky T 2014 *Nat. Phys.* **10** 39
- [19] Chen B G-G, Upadhyaya N and Vitelli V 2014 *Proc. Natl Acad. Soc.* **111** 13004
- [20] Paulose J, Chen B G and Vitelli V 2015 *Nat. Phys.* **11** 153
- [21] Huber S D 2016 *Nat. Phys.* **12** 621
- [22] Rechtsman M C, Zeuner J M, Plotnik Y, Lumer Y, Podolsky D, Dreisow F, Nolte S, Segev M and Szameit A 2013 *Nature* **496** 196
- [23] Lu L, Joannopoulos J D and Soljačić M 2016 *Nat. Phys.* **12** 626
- [24] Agulló-Rueda F, Mendez E E and Hong J M 1989 *Phys. Rev. B* **40** 1357
- [25] Kim N Y, Kusudo K, Wu C, Masumoto N, Löffler A, Höfling S, Kumada N, Worschech L, Forchel A and Yamamoto Y 2011 *Nat. Phys.* **7** 681
- [26] Sun K, Gu Z, Katsura H and Das Sarma S 2011 *Phys. Rev. Lett* **106** 236803
- [27] Chern G-W, Chien C-C and Di Ventra M 2014 *Phys. Rev. A* **90** 013609
- [28] Shen S-Q 2013 *Topological Insulators: Dirac Equation in Condensed Matters* (Berlin: Springer)